Journal of the Serbian Chemical Society
JSCS-info@shd.org.rs • www.shd.org.rs/JSCS
J. Serb. Chem. Soc. *85* (10) 1317–1328 (2020)
JSCS–5377
UDC 620.193:546.46AZ91D:544.654.2+544.72.023
Original scientific paper

Corrosion protection of AZ91D magnesium alloy by a duplex coating

ANA D. FORERO LÓPEZ[1], ANA P. LOPERENA[1], IVANA L. LEHR[1]*
LORENA I. BRUGNONI[2] and SILVANA B. SAIDMAN[1]

[1]*Chemical Engineering Department, Institute of Electrochemical and Corrosion Engineering, National University of the South, CONICET, Bahía Blanca, Argentina and* [2]*Department of Biology, Biochemistry and Pharmacy, Institute of Biological and Biomedical Sciences, National University of the South, CONICET, Bahía Blanca, Argentina*

(Received 21 February, revised 3 May, accepted 19 May 2020)

Abstract: A duplex coating was formed under potentiostatic conditions on magnesium alloy AZ91D in order to improve its corrosion resistance in a simulated physiological environment. The first layer was formed by anodization at low potentials in molybdate solution. The outer layer was a PPy film electrosynthesized in sodium salicylate solution. The conditions of the formation were determined to obtain a layer with globular morphology. The bilayer was characterized by scanning electron microscopy (SEM) and X-ray diffraction (XRD). The corrosion protection properties of the coatings were examined in Ringer solution by monitoring the open circuit potential (OCP), polarization techniques, and electrochemical impedance spectroscopy (EIS). The obtained results showed that the bilayer improves the corrosion resistance of the substrate. Moreover, the duplex coating presented better anticorrosive properties than a single PPy film. Afterwards, the bilayer was modified by cementation of silver ions from a solution containing $AgNO_3$. The modified electrode exhibited good antibacterial properties.

Keywords: Mg substrate; anticorrosion; electrodeposited polypyrrole; molybdate; salycilate.

INTRODUCTION

Nowadays, titanium are the common biocompatible materials used for biomedical implants. However, these metals release corrosion products that are harmful to human health.[1] This issue leads to the necessity of a second surgery to remove the implant in order to avoid infections. The removal surgery not only implies additional costs but also exposes the patient to a stressful and sometimes painful situations.[2] Thus, biodegradable materials have been studied for their use

* Corresponding author. E-mail: ilehr@uns.edu.ar
https://doi.org/10.2298/JSC200221027F

Available on line at www.shd.org.rs/JSCS/
(CC) 2020 SCS.

in the biomedical field. Magnesium alloys have attracted attention as orthopedic implants due to its similar mechanical properties to bone (as Young's modulus, light weight, tensile strength) and biodegradability.[3–5] These properties make Mg and its alloys attractive for the fabrication of temporary orthopedic implants such as bone plates, rods, screws, wires, joint replacements, and also for cardiovascular implants such as stents.[1,6] Under physiological conditions, magnesium corrodes and degrades completely. Mg is naturally presented in the human body, so it could be easily metabolized and excreted without causing any health damage.[1,7] Thus, Mg and its alloys are good alternatives as temporary implant materials, such as plates and raw materials, since, after the tissue heals, they will be corroded and eliminated from the body avoiding the necessity of a second surgery for implant removal. However, their fast degradation rate in the physiological environment leads to early loss of mechanical integrity and a high local pH value in the surrounding tissues, which are undesired for the use as implant materials.[4,5] Therefore, it is very important to improve the corrosion resistance of Mg alloys in order to ensure their suitability.

Conducting polymers are suitable materials for corrosion protection of metallic substrates, especially polypyrrole (PPy) due to its high stability,[8] good biocompatibility,[9] adhesion and interesting redox properties.[10] Several reports showed an improvement in the corrosion performance of Mg alloys by electrosynthesis of PPy coatings. The dissolution rate of Mg alloys is reduced in presence of salicylate solution.[11,12] For this reason, the anion is widely used as electrolyte for the electropolymerization of Py onto these materials.[11–14]

It was reported in previous works that electrosynthesis of PPy in salicylate solution leads to the formation of diverse structures. Hollow rectangular microtubes of polypyrrole were formed potentiostatically onto 316L stainless steel, onto nitinol and onto AZ91D Mg alloys in neutral and alkaline solutions of salicylate (Sa).[15–17] Electrodeposited PPy films with microtubular structure on the first layer were reported to be obtained by anodization of AZ91D alloy in molybdate solution.[17] The duplex coating shows an improved anticorrosive performance with respect to a PPy film. This improvement is associated with the combination of characteristics, such as the protective properties of the inner film, the ability of the polymer to maintain the metal in the passive state and the inhibitor characteristics of salicylate. The incorporation of silver particles into the duplex coating allowed the anticorrosive performance of the films to be increased. The Ag-modified bilayer also exhibited good antibacterial activity against *Escherichia coli*.

The main goals of the present work were to evaluate and improve the anticorrosive performance of PPy films with granular morphology electrosynthesized on AZ91D Mg alloy from a salicylate solution. In this regard, the polymer was deposited onto a film electroformed in molybdate solution. Electrochemical

(CC) 2020 SCS.

impedance spectroscopy (EIS) and other electrochemical techniques were used to study the inhibition ability of the films in simulated physiological solution. The coating remained protecting, stable and adherent during long exposure times. Silver-modified bilayer presented antibacterial activity.

EXPERIMENTAL

Materials and methods

A die-cast AZ91D magnesium alloy (composition, wt. %: 8.978 Al, 0.6172 Zn, 0.2373 Mn, 0.2987 Si, 0.1189 Cu, 0.00256 Ni, 0.017 Fe, 0.00164 Ca, 0.01154 Zr, balance Mg) was used as working electrodes. The samples were prepared from rods and embedded in a Teflon holder with an exposed area of 0.070 cm^2. The surface of the electrode was wet mechanically polished successively with 600 and 1000 grit finish using SiC before each experiment. After this process, the exposed surfaces were degreased with acetone and washed with triply distilled water. Following this pretreatment, the electrode was immediately transferred to the electrochemical cell. All the potentials were measured against a saturated Ag/AgCl electrode and a platinum sheet was used as a counter electrode. The cell was a 20 cm^3 Metrohm measuring cell.

The solutions were purified with a saturated atmosphere of nitrogen gas at 25 °C. Pyrrole (Py, Sigma–Aldrich) was freshly distilled under reduced pressure before use. All chemicals were reagent grade and solutions were made double distilled water.

Electrochemical measurements were performed using a potentiostat–galvanostat Autolab/PGSTAT 128N and VoltaLab40 Potentiostat PGZ301. An EVO 40 XVP (LEO) microscope, with an accelerating voltage of 20 keV was used to examine surface morphology of coatings. X-Ray diffraction analysis (XRD) was performed using a Rigaku X-ray diffractometer (model Dmax III-C) with Cu K_α radiation and a graphite monochromator. Film adhesion was tested by measuring the force necessary to peel-off the film using a Scotch® MagicTM double coated Tape 810 (3M) and a Mecmesin basic force gauge (BFG 50N).

The variation of the open circuit potential (*OCP*) as a function of time, potentiodynamic method and electrochemical impedance spectroscopy (EIS) were used to evaluated the corrosion behavior in Ringer solutions at 37 °C. The composition of Ringer solution is (per liter) 8.60 g NaCl, 0.30 g KCl and 0.32 g $CaCl_2 \cdot 2H_2O$. The electrodes were allowed to equilibrate at the fixed voltage before the ac measurements.

The Tafel tests were performed by polarizing from cathodic to anodic potentials with respect to the open circuit potential at 0.001 V s^{-1} in Ringer solution. Estimation of corrosion parameters was realized by the Tafel extrapolation method. The extrapolation of anodic and/or cathodic lines for charge transfer controlled reactions gives the corrosion current density (j_{corr}) at the corrosion potential (E_{corr}). Electrochemical impedance spectra were obtained at the open circuit potential (*OCP*) in the frequency range from 100 kHz to 100 mHz, and the signal amplitude was 10 mV. Furthermore, the EIS data were analyzed and modeled into equivalent electrical circuits (EEC) with Z-View software. All experiments were conducted after the steady-state E_{corr} was attained. The measurements were repeated four times for each investigated coating to ensure reproducible and significant data.

The antibacterial activity against the Gram-negative bacteria *Escherichia coli* was evaluated by a modified Kirby–Bauer technique.[18] The method was previously standardized by adjusting the microbial inoculation rate and the volume of the agar medium layer. A stock culture of *E. coli* ATCC 25922 (stored at –70 °C in Tripticase Soy Broth (TSB) (BK 046HA, Biokar Diagnostics) supplemented with 20 vol. % glycerol (Biopack, Argentina) was used. A loop of frozen cells was cultured in TSB during 24 h at 37 °C, harvested by centrifugation at

(CC) 2020 SCS.

5000*g* for 10 min (Labofuge 200, Kendro, Germany), washed twice with phosphate-buffered saline (PBS: 0.15 mol l^{-1} NaCl, 0.05 mol l^{-1} KH_2PO_4, 0.05 mol l^{-1} K_2HPO_4, pH 7.2) and then, cell pellets were suspended in PBS to achieve a population of *ca*. 7.0 log *CFU* (colony forming units) ml^{-1} using a spectrophotometer (Thermo Spectronic Genesys 20, Thermo Electron Corporation, MA, USA). One milliliter of this suspension was mixed with 25 mL of Muller–Hinton Agar (BK, Biokar Diagnostics) melted and cooled at 43 °C, and then, placed on a Petri dish. The coated electrodes were pressed onto bacteria-overlaid agar and incubated at 37 °C for 48 h. The data is expressed as growth inhibitory zone diameter (mm) for three replicates.

RESULTS AND DISCUSSION

Polypyrrole coatings

The PPy film was easily formed by electrochemical anodic oxidation from a sodium salicylate (NaSa) solution containing the monomer. It was reported that hollow rectangular microtubes of PPy were electrodeposited on AZ91D Mg alloy in a solution containing 0.50 M NaSa and Py.[17] The typical PPy globular structure was generated for lower NaSa concentrations. The *i*–*t* curves obtained for AZ91D Mg alloy at 1.15 V during 600 s in a solution containing 0.50 M NaSa and 0.50 M Py are shown in Fig. 1A and those obtained at 0.80 V during 1800 s in a solution containing 0.10 M NaSa and 0.25 M Py are shown in Fig. 1B.

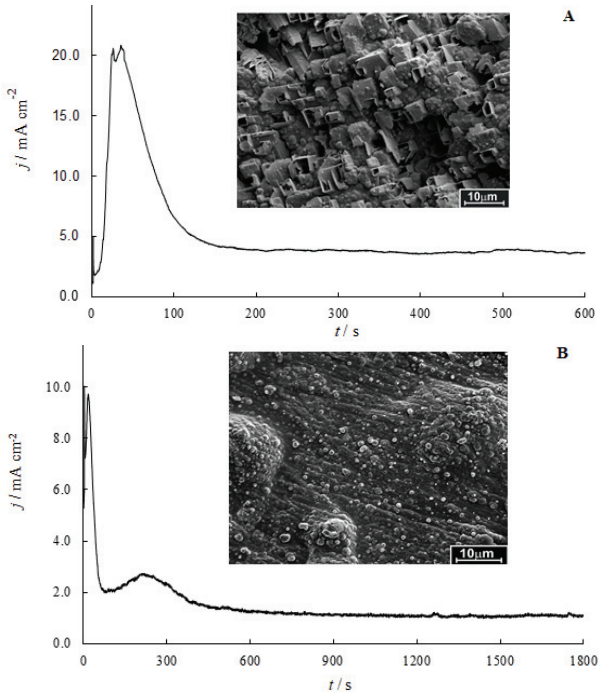

Fig. 1. Chronoamperometric curves obtained during the electrosynthesis of: A – $PPy_{0.50}$ and B – $PPy_{0.25}$ films. SEM images of the films are also presented.

(CC) 2020 SCS.

SEM images of the obtained films are also shown in the Fig. 1. Rectangular microtubes of PPy were formed in the solution with the higher Sa content, while a granular PPy morphology was obtained for the lower Sa concentration. The coatings will be called $PPy_{0.5}$ and $PPy_{0.25}$, respectively. Higher current densities were registered during the formation of the microtubular structures, but the samples were prepared by using the same electropolymerization charge.

The potentiodynamic polarization plots recorded for the bare sample and the alloy covered by the $PPy_{0.25}$ and $PPy_{0.5}$ coatings are compared in Fig. S-1 of the Supplementary material to this paper. The increase in the anodic current density registered for the uncoated electrode is related to active dissolution of the alloy. As it can be observed, the presence of both coatings produces a displacement of the onset potential, reaching a more positive value in the case of $PPy_{0.25}$. This result can be explained by considering that the porosity of the microtubular $PPy_{0.5}$ coating allows an easier diffusion of corrosive ions to the electrode surface. The more compact globular coating leads to an increased corrosion resistance. Then, it was decided to improve the corrosion protection imparted by the $PPy_{0.25}$ film.

Bilayer coating

A protective film was generated onto AZ91D Mg alloy in a molybdate solution[17]using a low-voltage anodizing method. In order to improve the corrosion resistance of the AZ91D alloy, a bilayer was prepared by first applying anodization to modify the substrate, and then depositing a $PPy_{0.25}$ film. For simplification, the coating will be named RMo–$PPy_{0.25}$. The bilayered system with the best performance was obtained when the substrate was anodically polarized at 1.0 V in 0.25 M Na_2MoO_4 solution during 20 s. After this treatment, the PPy film was electrosynthesized at 0.80 V during 1800 s in an electrolyte solution containing 0.10 M NaSa and 0.25 M Py. A SEM image shows that the globular polymeric film covers the electrode surface (Supplementary material, Fig. S-2).

If the potentiodynamic polarization curves of the alloy covered by $PPy_{0.25}$ and RMo–$PPy_{0.25}$ in Ringer solution are compared, it could be notice that the bilayer provides better corrosion protection (Fig. S-3, curve c).

The *OCP* of the alloy covered by RMo–$PPy_{0.25}$ was measured in Ringer solution over a period of 30 h (Fig. S-4). The immersion time was shorter for the bare and $PPy_{0.25}$-covered electrode because of the high corrosion rate of these samples. The alloy covered by the $PPy_{0.25}$ revealed a continuous potential decrease until the corrosion potential of the bare alloy was attained after 6 h of immersion (Fig. S-4, curve b). In contrast, the *OCP* for the RMo–$PPy_{0.25}$ was more positive than that of the untreated alloy, even after a long period of immer-

(CC) 2020 SCS.

sion (Fig. S-4, curve c). Moreover, there was no sign of corrosion damage visible to the naked eye for this bilayer coated sample after the *OCP* experiment.

After 5 h of immersion of the alloy samples, the Ringer solution was analyzed to determine the Mg concentration. The released amount of Mg by the untreated alloy was 3.90 mg L^{-1}, whereas it was 2.10 mg L^{-1} for the $PPy_{0.25}$--covered sample. The concentration diminished to 1.81 mg L^{-1} in the case of RMo–$PPy_{0.25}$.

Representative Tafel plots obtained for the different samples in Ringer solution are presented in Fig. 2. The curves show qualitatively similar behaviour but with different values of their electrochemical data. The corresponding corrosion parameters are presented in Table I. $PPy_{0.25}$ and RMo–$PPy_{0.25}$ caused a positive displacement in the corrosion potential relative to the value of the bare alloy. The highest potential shift of about 0.350 V was observed for the RMo–$PPy_{0.25}$--covered sample. It can be also seen that the corrosion current density of the RMo–$PPy_{0.25}$ coated specimen becomes one order of magnitude lower than that for the uncoated alloy.

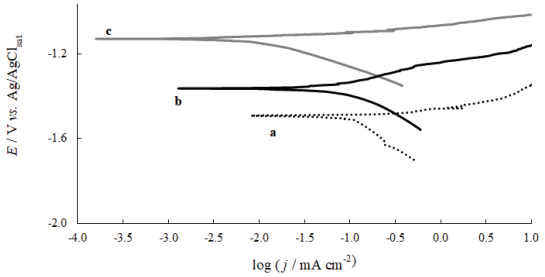

Fig. 2. Tafel curves obtained in Ringer solution after 60 min of immersion for: a) uncoated alloy and the alloy covered with: b) $PPy_{0.25}$ and c) RMo–$PPy_{0.25}$.

TABLE I. Corrosion parameters calculated from Tafel polarization plots for the uncoated alloy and the alloy covered with $PPy_{0.25}$ and RMo–$PPy_{0.25}$. The mean values and their standard deviation are presented

Sample	E_{corr} / V	j_{corr} / mA cm^{-2}	b_a / V dec^{-1}	b_c / V dec^{-1}
AZ91D	–1.501 ± 0.050	0.1050 ± 0.0050	0.045	–0.293
$PPy_{0.25}$	–1.363 ± 0.030	0.0589 ± 0.0050	0.107	–0.142
RMo–$PPy_{0.25}$	–1.150 ± 0.020	0.0174 ± 0.0050	0.055	–0.128

EIS was used to evaluate the corrosion behavior of uncoated (Fig. 3A) and RMo–$PPy_{0.25}$ coated Mg alloy (Fig. 3B) in Ringer solution under open circuit conditions. The impedance spectra of the coated substrate obtained during different immersion times is presented. The Nyquist plot of the bare sample after 2 h of immersion is characterized by two overlapping capacitive semicircles followed

(CC) 2020 SCS.

by an inductive loop. The impedance of the coated sample is higher than that of the bare alloy, indicating the good corrosion protection imparted by the coating.

In order to analyze the results in more detail, the EIS data were fitted with the equivalent circuits proposed in the literature for magnesium alloys immersed in chloride-containing solutions (Fig. S-5A),[20,21] as well as for metallic materials coated by PPy films (Fig. S-5B).[22] The equivalent circuits make use of a constant phase element (CPE) as a substitute for a capacitor. The fitting data are listed in Table II. The model simulates the experimental data well, considering that the errors of fitting were lower than 5 % for all the parameters.

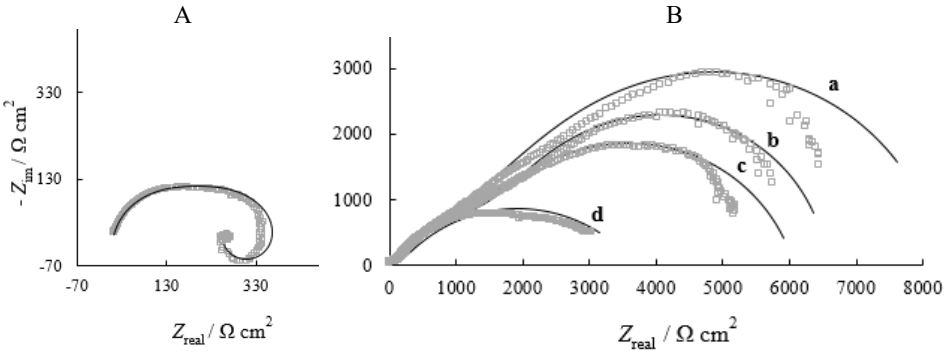

Fig. 3. Nyquist plot for: A – uncoated alloy registered at the *OCP* in Ringer solution after 2 h of immersion and B – the RMo–PPy$_{0.25}$-coated alloy registered at the *OCP* in Ringer solution after immersion during: a – 2, b – 5, c – 8 and d – 24 h; (□) experimental data; (–) fitted data.

TABLE II. Values for the parameters of the equivalent circuit obtained from the best fit to the impedance data

Parameter	AZ91D	RMo–PPy$_{0.25}$			
t / h	2	2	5	8	24
R_s / Ω cm^2	11.33	–	–	–	–
R_0 / Ω cm^2	–	26.6	24.5	26.0	12.0
C / F cm^{-2}	–	6.43×10^{-8}	7.14×10^{-8}	6.35×10^{-8}	8.28×10^{-8}
R_1 / Ω cm^2	243.60	116.97	91.53	93.63	81.08
R_2 / Ω cm^2	162.2	2145	2040	1550	3498
CPE_1, F / cm^{-2}	2.14×10^{-4}	–	–	–	–
n	0.79	–	–	–	–
CPE_2, F / cm^{-2}	4.08×10^{-5}	2.12×10^{-5}	1.98×10^{-5}	1.98×10^{-5}	8.74×10^{-5}
n	0.86	0.64	0.63	0.63	0.58
R_3 / Ω cm^2	–	5645	4434	4413	77
CPE_3, F / cm^{-2}	–	2.07×10^{-5}	3.30×10^{-5}	3.14×10^{-5}	1.44×10^{-5}
n	–	0.93	0.95	0.83	0.70
L / H	700	–	–	–	–

In the case of the equivalent circuit proposed for the bare sample, R_s is the solution resistance, CPE_1 and R_1 represent the capacitance and resistance of the

(CC) 2020 SCS.

surface film, respectively. CPE_2 and R_2 are related to the double layer capacitance and the charge transfer resistance at the surface of the alloy. The inductance (L) is attributed to the presence of adsorbed/desorbed intermediates or other species on the bare surface of the sample.[23,24]

In the equivalent circuit proposed for the coated sample, R_0 is the sum of the electrolyte solution and polymer film resistances. R_1 and C_1 represent, respectively, the pore resistance and the capacitance of the coating. CPE_2 and R_2 are related to the charge transfer of the reaction between the PPy film and the substrate. Finally, CPE_3 and R_3 represent the interface between RMo and the substrate.

It could be observed that the fitted values of the capacitive components in the circuit remained nearly constant with immersion time. It was postulated that galvanic coupling of the polymer to the substrate contributes to oxidization of the substrate forming a passive film. The slow decrease in the R_2 values with time may indicate that the reaction between the PPy film and the substrate is not inhibited. In spite of part of the polymer matrix being reduced, its resistance (R_0) remained unaltered. The decrease in the R_3 values could be interpreted as the result of a progressive dissolution of the RMo film.[20]

The obtained results suggest that anodization in molybdate solution helps in maintaining the alloy in a more passive state. On the other hand, the RMo––$PPy_{0.25}$ coating has a better adhesion than the $PPy_{0.25}$ film (Table III).

TABLE III. Adherence force obtained for the different coatings after peel-off testing

Sample	Adherence force, N
PPy0.25	16.25
RMo–$PPy_{0.25}$	21.70
RMo–$PPy_{0.25}$–Ag	12.95

Silver deposition

Another objective of this work was to study silver deposition on the bilayer coating. It is well known that metallic Ag can be spontaneously deposited on PPy. The RMo–$PPy_{0.25}$-covered electrodes were immersed in 0.05 M $AgNO_3$ solution for 4 h under open circuit conditions. As seen in Fig. S-6, the RMo––$PPy_{0.25}$-covered sample shows a deposit of silver platelets.

The XRD spectra for coated and uncoated AZ91D Mg alloy are shown in Fig. 4. XRD analysis of the coating confirmed the presence of silver. Two intense diffraction peaks detected at 2θ values of 38.14 and 44.34° correspond to the Bragg reflections of Ag (111) and (200) the planes.[25]

The amount of Ag was higher for RMo–$PPy_{0.5}$[17] than for RMo–$PPy_{0.25}$. This could be related to the higher surface area of the microtubular polymer in

(CC) 2020 SCS.

contact with the $AgNO_3$ solution and also to the higher amount of available Sa anions.

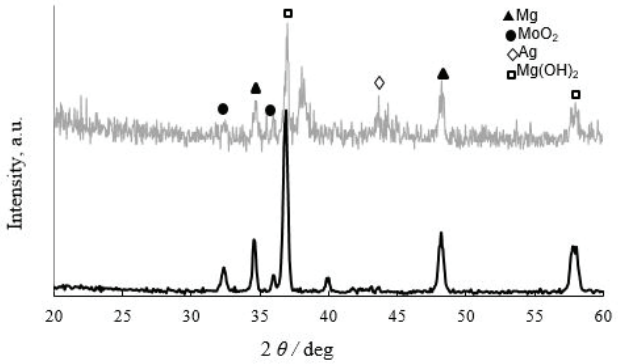

Fig. 4. XRD spectrum for: a – uncoated alloy and b – the alloy covered with RMo–$PPy_{0.25}$–Ag.

By comparing the XRD patterns of both samples, it could also be concluded that the coated sample presents diffraction peaks corresponding to the substrate. Peaks of MoO_2 are also observed. There are no peaks corresponding to MoO_3 although the presence of amorphous MoO_3 should not be dismissed.[26,27] The polarization curve indicates that active dissolution of the substrate shifts to appreciably nobler values after Ag deposition (Fig. S-3, curve c). Thus, according to this result, silver deposition significantly improved the corrosion resistance property of the bilayered coating.

The OCP variation with time for the Ag-modified sample exposed to Ringer solution is presented in Fig. S-4, curve d. Except for the first hours of immersion, the corrosion potential is near to the value of the bare alloy. On the other hand, the quantity of Mg released is practically the same as that obtained with the bilayered coating (1.81 mg L^{-1}).

Tafel plots for the sample covered by the Ag-modified coating were not reproducible. In spite of this, the i_{corr} values were always around that corresponding to the RMo–$PPy_{0.5}$-covered sample.

The Ag-modified coatings were compact but their adhesion to the substrate surface was poor (Table III). The bad protection against alloy corrosion for long immersion times as well as the irreproducibility in some measurements could be explained considering the poor adherence of the coating. Research is on-going in order to improve the degree of adhesion.

The antibacterial activity of immobilized silver against the Gram-negative bacteria *E. coli* ATCC 25922 was investigated by determining the width of the inhibition zone around the coated surfaces. The RMo–$PPy_{0.25}$ film did not inhibit the growth of the bacteria but an inhibition zone with a mean value of 14 mm was

(CC) 2020 SCS.

observed in the case of the RMo–$PPy_{0.25}$–Ag coating. The presence of inhibition zones indicates the release of silver to the surrounding environment and subsequent antimicrobial effect. The antibacterial activity of RMo–$PPy_{0.25}$–Ag films could be explained by the penetration of the released Ag^+ and colloidal silver particles through the bacteria cell wall. Their complexation with enzymes in the cell membrane results in the inhibition of the enzymatic activity and death of the bacteria.[28]

CONCLUSIONS

A PPy film with granular morphology electrodeposited onto AZ91D Mg alloy in Sa solution presents better anticorrosive properties than the same polymer with microtubular morphology. In order to improve the corrosion behavior of the substrate, the globular polymer was deposited on top of a film electroformed in molybdate solution. The bilayer system had a valuable effect on lowering the corrosion current density of the alloy in Ringer solution. The coating remained protecting, stable and adherent during long exposure times. Silver deposition was performed on the duplex coating under *OCP* conditions. Preliminary results indicate that this film has antibacterial activity.

SUPPLEMENTARY MATERIAL

Additional data are available electronically from the journal web site: http://www.shd.org.rs/JSCS/, or from the corresponding author on request.

Acknowledgements. CONICET (PIP-112-201101-00055), ANPCYT (PICT-2015- 0726) and Universidad Nacional del Sur (PGI 24/M127), Bahía Blanca, Argentina are acknowledged for financial support.

И З В О Д

ЗАШТИТА ОД КОРОЗИЈЕ ЛЕГУРЕ МАГНЕЗИЈУМА AZ91D ПРИМЕНОМ ДУПЛЕКС ПРЕВЛАКЕ

ANA D. FORERO LÓPEZ[1], ANA P. LOPERENA[1], IVANA L. LEHR[1], LORENA I. BRUGNONI[2] и SILVANA B. SAIDMAN[1]

[1]*Chemical Engineering Department, Institute of Electrochemical and Corrosion Engineering, National University of the South, CONICET, Bahía Blanca, Argentina u* [2]*Department of Biology, Biochemistry and Pharmacy, Institute of Biological and Biomedical Sciences, National University of the South, CONICET, Bahía Blanca, Argentina*

Дуплекс превлака је формирана под потенциостатским услоовима на легури магнезијума AZ91D у циљу побољшања њене корозионе отпорности у симулираној физиолошкој средини. Први слој је формиран анодизацијом на ниским потенцијалима у раствору молибдата. Спољашњи слој је био филм полипирола (PPy) који је синтетисан из раствора натријум-салицилата. Услови за формирање су подешени тако да се добије слој глобуларне морфологије. Двоструки слој је карактерисан скенирајућом електронском микроскопијом (SEM) и дифракцијом X-зрака (XRD). Ефикасност корозионе заштите превлака је испитивана у Рингеровом раствору праћењем потенцијала отвореног кола, поларизационим мерењима и спектроскопијом електрохемијске импеданције. Добијени резултати су показали да да двоструки слој побољшава корозиону отпорност подлоге. Штавише, дуплекс превлака је показала боља антикорозиона својства од једнослојне

(CC) 2020 SCS.

превлаке PPy. На крају, двоструки слој је модификован цементацијом јона сребра из раствора који је садржао $AgNO_3$. Модификована електрода је показала добра антибактеријска својства.

(Примљено 13. фебруара, ревидирано 13 маја, прихваћено 19. маја 2020)

REFERENCES

1. V. K. Bommala, M. G. Krishna, C. T. Rao, *J. Magnes. Alloy*. **7** (2019) 72 (https://doi.org/10.1016/j.jma.2018.11.001)
2. M. Sankar, J. Vishnu, M. Gupta, G. Manivasagam, *Applications of Nanocomposite Materials in Orthopedics*, Elsevier Inc., Ámsterdam, 2019, pp. 83–109 (https://doi.org/10.1016/B978-0-12-813740-6.00005-3)
3. F. Witte, V. Kaese, H. Haferkamp, E. Switzer, A. Meyer-Linderberg, C. J. Wirth, H. Windhagen, *Biomaterials* **26** (2005) 3557 (https://dx.doi.org/10.1016/j.biomaterials.2005.10.003)
4. Z. Zhai, X. Qu, H. Li, K. Yang, P. Wan, L. Tan, Z. Ouyang, X. Liu, B. Tian, F.Xiao, W. Wang, C. Jiang, T. Tang, Q. Fan, A. Qin, K. Dai, *Biomaterials* **35** (2014) 6299 (https://dx.doi.org/10.1016/j.biomaterials.2014.04.044)
5. P. Amaravathy, S. Sathyanarayanan, S. Sowndarya, N. Rajendran, *Ceram. Int.* **40** (2) 6617 (https://dx.doi.org/10.1016/j.ceramint.2013.11.119)
6. A. Chaya, S. Yoshizawa, K. Verdelis, N. Myers, B. J. Costello, D. T. Chou, S. Pal, S. Maiti, P. N. Kumta, C. Sfeir. *Acta Biomater*. **18** (2015) 262 (https://doi.org/10.1016/j.actbio.2015.02.010)
7. N. Sezer, Z. Evis, S. M. Kayhan, A. Tahmasebifar, M. Koç. *J. Magnes. Alloys* **6** (2018) 23 (https://doi.org/10.1016/j.jma.2018.02.003)
8. D. J. Walton, *Mater. Des.* **11** (1990) 142 (https://dx.doi.org/10.1016/0261-3069(90)90004-4)
9. N. K. Guimard, N. Gomez, C. E. Schmidt, *Prog. Polym. Sci*. **32** (2007) 876 (https://dx.doi.org/10.1016/j.progpolymsci.2007.05.012)
10. D. Gopi, S. Ramya, D. Rajeswari, L. Kavitha*, Colloids Surfaces, B* **107** (2013) 130 (https://dx.doi.org/10.1016/j.colsurfb.2013.01.065)
11. M. C. Turhan, M. Weiser, H. Jha, S. Virtanen, *Electrochim. Acta* **56** (2011) 5347 (https://dx.doi.org/10.1016/j.electacta.2011.03.120)
12. M. C. Turhan, M. Weiser, M. S. Killian, B. Leitner, S. Virtanen, *Synth. Met*. **161** (2011) 360 (https://dx.doi.org/10.1016/j.synthmet.2010.11.048v)
13. Z. Grubač, I. Š. Rončević, M. M. Huković, *Corros. Sci*. **102** (2016) 310 (https://dx.doi.org/10.1016/j.corsci.2015.10.022)
14. M. Hatami, M. Saremi, R. Naderi, *Prog. Nat. Sci. Mat. Int.* **25** (2015) 478 (https://dx.doi.org/10.1016/j.pnsc.2015.10.001)
15. M. B. González, O. V. Quinzani, M. E. Vela, A. A. Rubert, G. Benítez, S. B. Saidman, *Synth. Met.* **162** (2012) 1133 (https://dx.doi.org/10.1016/j.synthmet.2012.05.013)
16. M. Saugo, D. O. Flamini, L. I. Brugnoni, S. B. Saidman, *Mater. Sci. Eng., C* **56** (2015) 95 (https://dx.doi.org/10.1016/j.msec.2015.06.014)
17. A. Forero López, I. L. Lehr, L. I. Brugnoni, S. B. Saidman, *J. Magnes. Alloys* **6** (2018) 15 (https://dx.doi.org/10.1016/j.jma.2017.12.005)
18. Clinical Laboratory Standards Institute**,** *Performance standards for antimicrobial disk susceptibility tests*, Approved standard – 9th ed., CLSI document M2-A9. 26:1, Clinical Laboratory Standards Institute, Wayne, PA, 2006

(CC) 2020 SCS.

19. A. Forero López, I. L. Lehr, S. B. Saidman, *J. Alloys Compd.* **702** (2017) 338 (https://dx.doi.org/10.1016/j.jallcom.2017.01.030)
20. S. Kaabi Falahieh Asl, S. Nemeth, M. Jen Tan, *Mater. Chem Phys*. **161** (2015) 185 (https://dx.doi.org/10.1016/j.matchemphys.2015.05.035)
21. F. Guadarrama-Muñoz, J. Mendoza-Flores, R. Duran-Romero, J. Genesca, *Electrochim. Acta* **51** (2006) 1820 (https://dx.doi.org/10.1016/j.electacta.2005.02.144)
22. K. Cysewska, L. Fernández Macía, P. Jasinski, A. Hubin, *Electrochim. Acta* **245** (2017) 327 (https://dx.doi.org/10.1016/j.electacta.2017.05.172)
23. M. Jamesh, S. Kumar, T. S. N. Sankara Narayanan, *Corros. Sci*. **53** (2011) 645 (https://dx.doi.org/10.1016/j.corsci.2010.10.011)
24. T. Ishizaki, Y. Masuda, K. Teshima, *Surf. Coat. Technol*. **217** (2013) 76 (https://dx.doi.org/10.1016/j.surfcoat.2012.11.076)
25. JCPDS, International Center of Powder Diffraction Data: Swarthmore, PA, 1989; Card No. 04-0783
26. T. M. McEvoy, K. J. Stevenson, *Langmuir* **19** (2003) 4316 (https://dx.doi.org/10.1021/la027020u)
27. A. Quintana, A. Varea, M. Guerrero, S. Suriñach, M. D. Baró, J. Sort, E. Pellicer, *Electrochim. Acta* **173** (2015) 705 (https://dx.doi.org/10.1016/j.electacta.2015.05.112)
28. T. Nonaka, Y. Uemura, K. Enishi, S. Kurihara, *J Appl. Polym. Sci.* **62** (1996) 1651 (https://dx.doi.org/10.1002/(SICI)1097-4628(19961205)62:10<1651::AID-APP17>3.0.CO;2-4).

(CC) 2020 SCS.